



Microstructure evolution and microhardness of friction stir welded cast aluminum bronze



Mostafa Saboktakin Rizi*, Amir Hossein Kokabi

Department of Materials Science and Engineering, Sharif University of Technology, Azadi Ave, P.O. Box 11365-9466, Tehran, Iran

ARTICLE INFO

Article history:

Received 26 July 2013

Received in revised form 5 February 2014

Accepted 11 February 2014

Available online 27 February 2014

Keywords:

Aluminum bronze

FSW

Microstructure

Grain size

Microhardness

ABSTRACT

Microstructural characteristics and mechanical properties of a friction stir welded cast aluminum bronze (Cu–9Al–1Fe), produced by a sand casting method, have been investigated at tool rotation of 850–1500 rpm and traverse speed of 50–100 mm/min. Refinement of the primary coarse cast microstructure in the base metal was seen after friction stir welding. Microstructure of the stir zone was characterized in four distinct areas of non-isometric fine grains while a significant grain growth was noticed in some of the areas. Conditions of grain growth are defined with high heat input intensity and low heat transfer capability. The grain size was observed to decrease after FSW, resulting in a greater microhardness across the welded region from about 100 HV in the base metal to about 150 HV at the center of the stir zone. The increased hardness in the stir zone may have stemmed from the locally refined grain size according to Hall–Petch relation.

© 2014 Elsevier B.V. All rights reserved.

1. Introduction

Aluminum bronze alloys are copper-based alloys in which the Al is added to the mixture up to 12% as the main alloying element [Copper Development Association \(1988\)](#), with the other major alloying elements being Ni, Fe, Mg and Si ([Callcut, 2002](#)). Aluminum bronze alloys are widely used in engineering components of marine applications due to the useful combination of good strength, wear and corrosion resistance ([Ni et al., 2010](#)), in addition to toughness and ductility ([Fuller et al., 2007](#)). However, aluminum bronzes which contain 10 wt% Al, solidify in 1030 °C as a single β -phase (bcc) due to an eutectic transformation. [Mishra et al. \(2007\)](#) and [Oh-ishi and McNelley \(2005\)](#) described that during a slow cooling, the β -phase will be transformed to both a α -phase (fcc) and an intermetallic γ -phase at lower temperatures through a eutectoid reaction. Further addition of iron to this compound will raise proportion of the α -phase allowing a greater amount of Al with no more γ -phase being formed. Meanwhile, the addition of Fe will form an intermetallic κ -phase within the microstructure. [Callcut \(2002\)](#) and [Ni et al. \(2009\)](#) noted that an additional amount of Fe in the compound will improve strength, fatigue strength and wear resistance.

Fusion welding of the cast aluminum bronze is usually employed to fabricate various components which are difficult to be produced as a single casting. It is also used to repair the casting defects. However, cracks, HAZ cracks, porosity and formation of brittle phase are some defects which can occur during fusion welding of the aluminum bronze. This is corroborated by the results of [Michael \(2006\)](#) and [Oh-ishi and McNelley \(2004\)](#). They showed that the friction stir welding is the best known technique to enhance both mechanical properties and microstructure of the welding in the aluminum bronze joints.

This article focuses on the microstructure evolution and mechanical properties of a cast aluminum bronze (Cu–9Al–1Fe) during FSW in a wide ranges of tools rotation (ω) and traverse speed (v). The purpose of this research is to determine the relationship between microhardness and microstructure of the aluminum bronze in addition to describe the microstructural changes in the welded zone.

2. Experimental

FSW technique was carried out on an as-cast aluminum bronze (UNS C 95,300) plates of 4 mm thickness. Chemical composition of this alloy is shown in [Table 1](#). Characteristics of the used welding tools were as follows: 16 mm diameter of a concave shoulder with a jagged pin of 3.8 mm length, with the other dimensions of this equipment being summarized in [Table 2](#). This tool design increases the contact surfaces between the pin and the plasticized

* Corresponding author. Tel.: +989378467621; fax: +989378467621.
E-mail address: saboktakin88@gmail.com (M.S. Rizi).

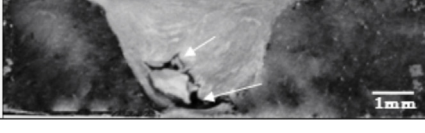
ω (rpm)	v (mm/min)	ω/v	ω^2/v	Macrostructural of the joints welded			Weld defects
				AS	Shoulder	RS	
1500	50	30	45000				Defect-free Weld
1250	50	25	31250				Defect-free Weld
1500	100	15	22500				Cavity
1250	100	12.5	15625				Cavity & Lack of penetration
850	50	17	14450				Cavity & Lack of penetration & Crack

Fig. 1. Macrostructure of the joints welded and defects at the various ω/v and ω^2/v ratios.

Table 1

Chemical composition of aluminum bronze used in the present study.

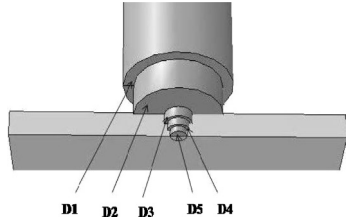
Element	Al	Fe	Cu	Other
Percent (%)	9.1	1	Balance	0.5

material (Gadakh and Adepu, 2013), thereby increasing the heat generation and providing a much easier flow of the plasticized material.

The tool itself is made of an air quenched AISI H13 hot worked tool steel. The rates of tools rotation (ω) and traverse speed (v) applied in the FSW of specimens are listed in Table 3. Using Optical Microscopy (OM) and Image Analysis software, microstructure and grain size of the base metal (BM), HAZ, TMAZ and several areas of the stir zone (SZ) were examined. Etching was performed in a (5 g) FeCl_3 + (2 ml) HCl + (95 ml) $\text{C}_2\text{H}_5\text{OH}$ solution (Ni et al., 2010), while microhardness was evaluated along vertical and cross-sectional areas of the weldment using a micro-Vickers hardness tester with 1 kg load for 15 s.

Table 2

Dimensions and schematic of the used tool.

	Shoulder		Pin			Schematic of tool
	D1	D2	D3	D4	D5	
Diameter (mm)	20	16	5	3.75	2.5	

3. Results and discussion

3.1. Macrostructure and microstructure

Arbegast and Hartley (1998) defined ω^2/v as a pseudo heat index, using an experimental viewpoint, and discussed the effect of it on heat input. The following proportion indicates the relation between; maximum temperature of the FSW process (T_{max} , °C), rotation rate (ω) and traverse speeds (v):

$$\frac{T_{\text{max}}}{T_{\text{melting}}} \propto \frac{\omega^2}{v}$$

It means that increasing the ω^2/v ratio leads to a higher welding temperature. Furthermore, it can be inferred that the variations of the tool rotation speed would have larger effects on the maximum temperature of process in comparison with the variations of the travel speed.

Arbegast (2008) demonstrated that the flow related defects occur at low temperature and cold FSW condition. It is postulated

Table 3
Tool rotation rates (ω) and traverse speeds (v) applied in FSW.

Rotation rate (rpm)	Traverse speeds (mm/min)
850	50
1250	50
1500	50
1500	100
1250	100

that the optimum processing conditions to prevent the flow related defects occur at a temperature with a sufficient flow rate.

Fig. 1 illustrates the macrostructure of the welded joints as well as the defects for different ω/v and ω^2/v ratios. The obtained results revealed that the ω^2/v ratio has a larger effect on the volume of the weld defects than ω/v ratio. Because of their low heat input, temperature and inadequate material flow, some defects were detected in the joints which were welded at smaller ω^2/v ratios ($<3 \times 10^3$ (rpm² × min)/mm) due to cavity defects, lack of penetration and crack. Reduction of the ω^2/v ratio from 22,500 to 14,450 may intensify occurrence of the defects, whereas increasing this ratio up to 3×10^3 will yield defect-free welds for the aluminum bronze.

The cast microstructures of aluminum bronzes have been illustrated in Fig. 2. At room temperature, the microstructure of this alloy contains α -phase with fcc lattice structure, martensite (β'), as well as κ (iv), κ (ii), and κ (i) phases. Of the four κ phases that can develop during an equilibrium cooling of the aluminum bronze alloys, the κ_i , κ_{ii} , and κ_{iv} phases are iron-rich, while the κ_{iii} phase is nickel-rich. The three iron-rich κ -phases having a DO3 lattice structure (Oh-ishi and McNelley, 2005) with Fe₃Al composition are those which can be formed by sand casting of the aluminum bronze. On the other hand, the κ (ii) and κ (i) phases are composed of dendritic particles with globular shapes (Fuller, 2006). Only the κ (iii)

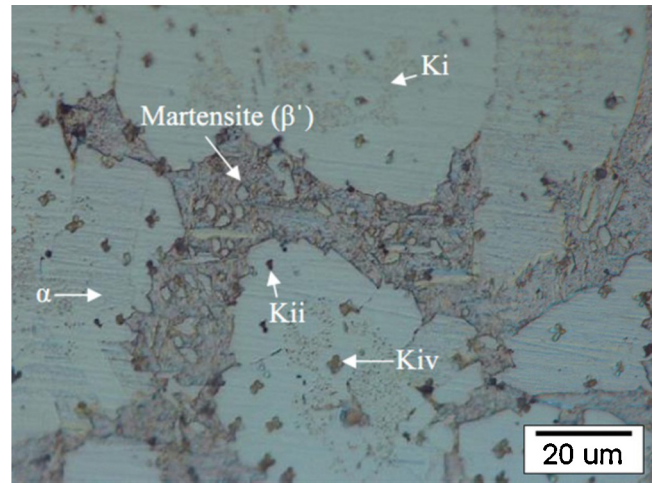


Fig. 2. Transformation products of β during cooling of cast microstructure.

phase was not observed during analysis of the processed aluminum bronze for this research, because the κ (iii) phase is nickel-rich and has been formed within microstructure of the nickel aluminum bronze alloys which were reported by Oh-ishi and Michael D. Fuller earlier.

Micrographs of the OM showing transverse sections of the stirred zones and microstructures of base metal (BM), heat affected zone (HAZ), thermo mechanical affected zone (TMAZ) and stirred zone (SZ) at a ω/v ratio of 1500/50 are depicted in Fig. 3. Four different microstructures were observed during welding of the aluminum bronzes within the cross-section, including the BM, HAZ, TMAZ and SZ. The interface between the SZ and the TMAZ was clearly sharp on the advancing side (AS), whereas it was not

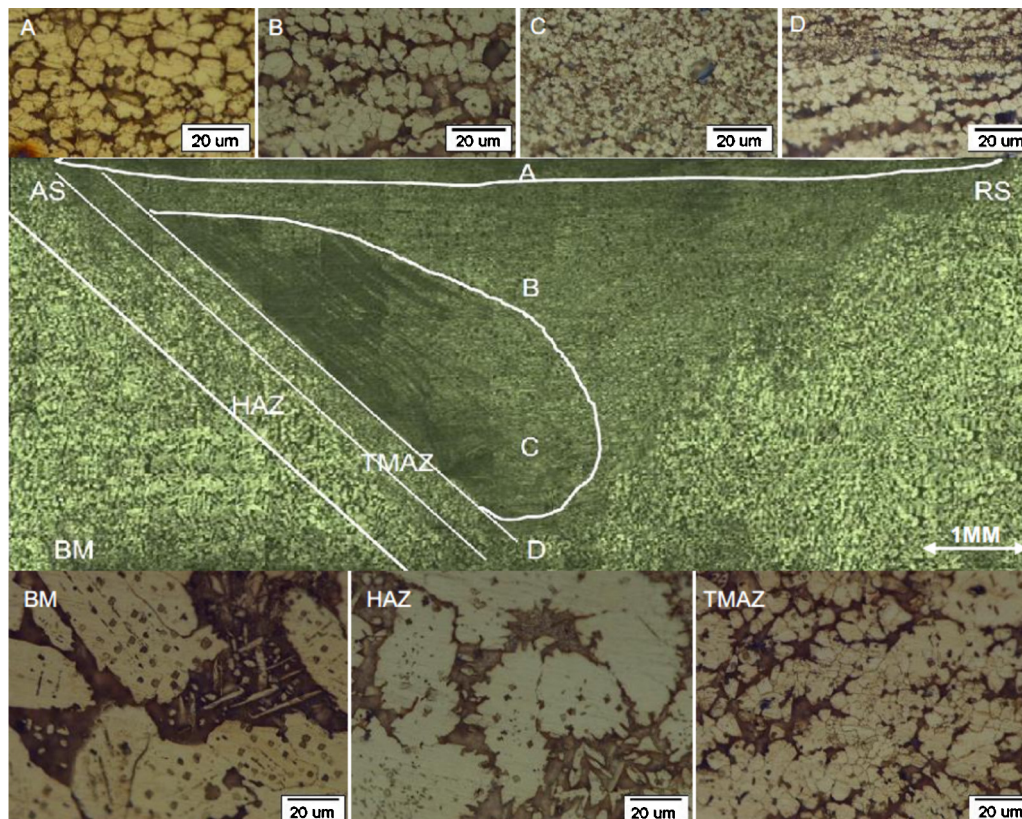


Fig. 3. Montages of optical micrographs and microstructure of BM, HAZ, TMAZ and four area of SZ (A–D) at 1500/50 (ω/v) ratio.

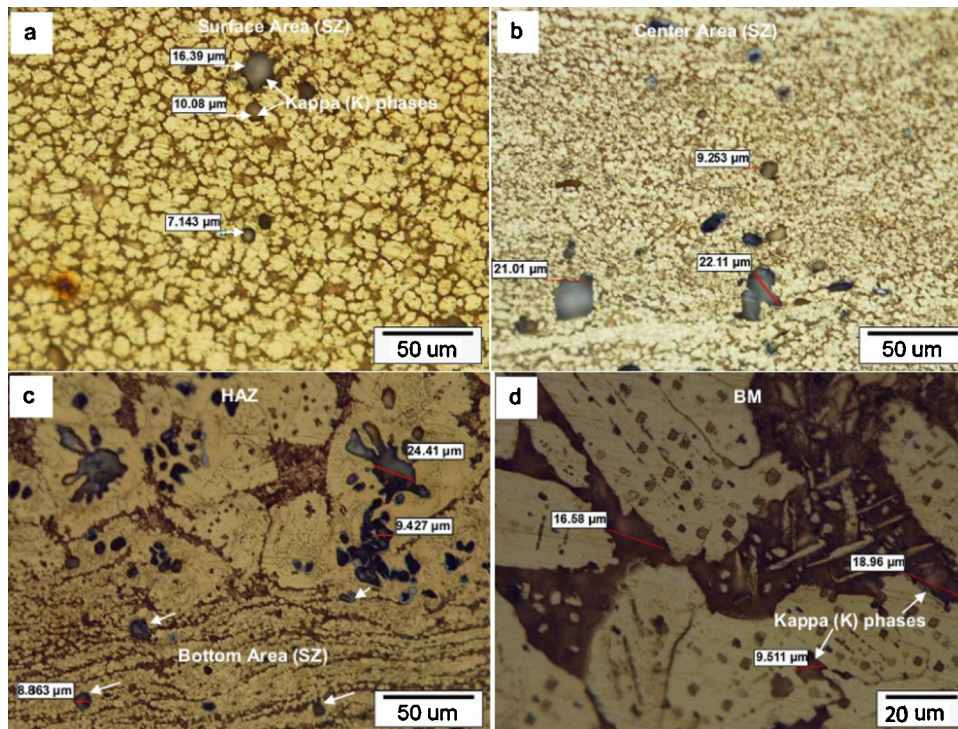


Fig. 4. Optical microscope images of: (a) surface area, (b) center area, (c) bottom area of stir zone and (d) BM at 1500/50 specimen.

sharp with a diffused feature on the retreating side (RS) and under the tool. Meanwhile, an onion-ring pattern was observed in the center of the SZ and close to the AS. Given the microstructures, the SZ could be divided into four areas from the surface to the bottom as shown in Fig. 3. Surface area (A) and subsurface (B) were associated with the equiaxed α grains due to the dynamic recrystallization resulting from a severe deformation. Stream like structure in center area (C) and bottom area (D) were elongated and generally aligned in the diagonal and horizontal directions,

respectively. In these microstructures, the bright areas were indicative of the α -phase whereas the darker ones referred to β' and κ -phases. The obtained results revealed that FSW was able to refine grain size and coarse microstructure of the casting.

As can be seen in Fig. 4, a comparison between the microstructures of the stir zone and the base metal for the specimens with ω/v of 1500/50 has uncovered presence of some globular particles in the size range of 7–25 μm , while size of the α grains decreases in the SZ. It implies that the κ -phase all through the stir zone (Figs. 4a–c)

Area \ ω/v	1500/50	1250/50	1500/100	1250/100
A				
B				
C				
D				

Fig. 5. Microstructure of quadruple areas of the specimen SZ in various ω/v ratios.

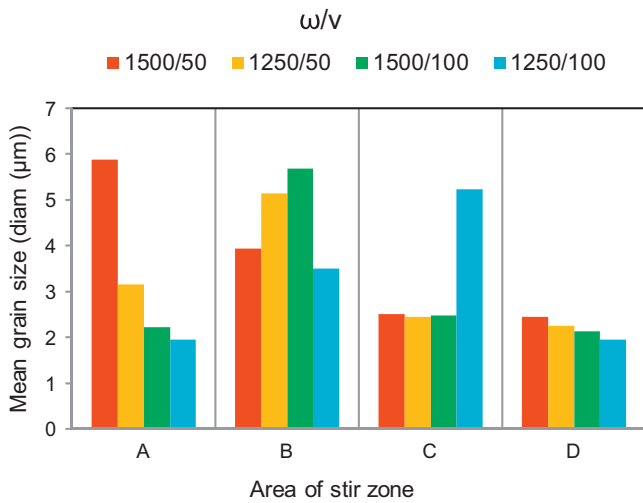


Fig. 6. Grain size of quadruple areas of the SZ of specimens in various ω/ν ratios.

was inconsistent with that of the base metal (Fig. 4d). Spherical shape of the particles could be attributed to the α-phase which is responsible for the full movement of these particles to the stirred zone during a FSW process.

As can be seen in Fig. 4c, a grain flow pattern is evident at the bottom of the stir zone; in the vicinity of the stir zone, and the material flow in this region indicates displacement direction of the globular particles.

3.2. Grain size

Within the SZ, four distinct areas with various equiaxed fine α-phase grains were distinguished starting from the surface down to the bottom areas. Comparisons between the microstructure and α grain size of the quadruplet SZ areas are presented in Figs. 5 and 6 for the specimens having different ω/ν ratios.

Increasing the tool rotation rate up to 1250–1500 rpm and simultaneously decreasing the traverse speed to 50 mm/min, led to a greater content of heat inputs which was associated with the ω/ν ratios, and also to a higher temperature of the FSW process that related to the ω²/ν ratios. The grain growing area was affected by temperature, heat input intensity and heat transfer of the process. By reducing the ω/ν ratios (from 1500/50 at 1250/100), this area was transferred from the surface area (A) to the subsurface (B) and central (C) areas. Since the required conditions for a higher heat transfer were met, some fine grain structures were formed across the bottom areas (D) in all the samples. Due to the high heat input, high temperature and low traverse speed, grain growth was obviously seen at the surface area (A) in the specimens of 1500/50 and 1250/50 ratios. When the traverse speed was increased, the heat had an insufficient time to be conducted ahead of the tool so that the material ahead of the tool was cold. Therefore, the inadequate conditions for grain growth after recrystallization has caused a fine grain size at the surface area (A) in the specimens associated with the 1500/100 and 1250/100 ratios. On the other hand, evolution of the grain growth was evident at the area (B) in all the specimens, perhaps due to high intensity of the heat input and low heat transfer in the subsurface area. However, grain growth was significant at the central area (C) of the specimen 1250/100 (Fig. 6).

3.3. Microhardness

Distribution of the micro-Vickers hardness along centerlines of the weldment cross-section is depicted in Fig. 7. Basically, the microhardness values across the SZ are typically higher than those

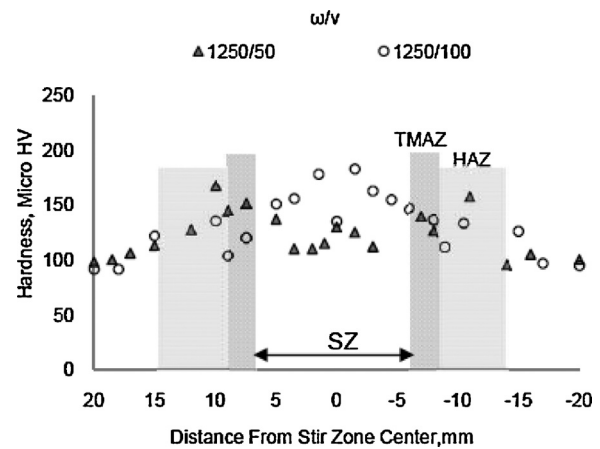


Fig. 7. Distribution of the micro-Vickers hardness along the centerlines on the cross-sections of the weldment.

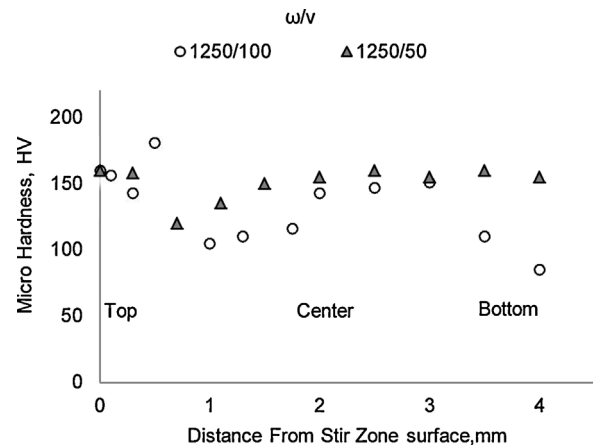


Fig. 8. vertical microhardness profiles across the SZ.

of the HAZ and BM. This hardness difference may be attributed to the fine grain size of the SZ as compared to the coarse grains of BM and HAZ.

Distribution profile of the Vickers hardness within the SZ is shown in Fig. 8. The relationship reveals a strong grain size dependence of the hardness in the weld zone. The obtained results revealed an inverse relationship between the values of grain size and hardness. In other words, the greater hardness of the

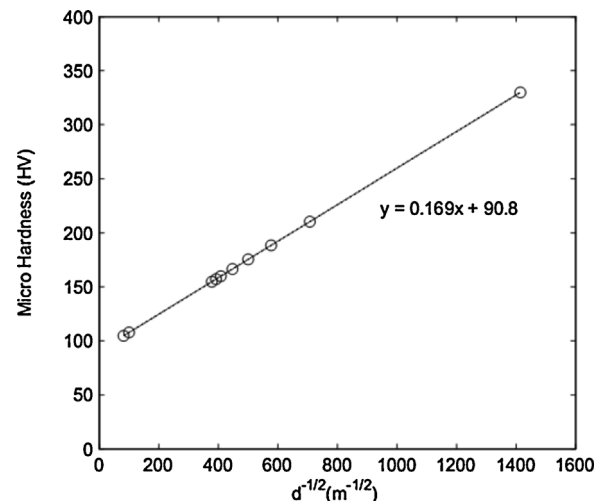


Fig. 9. Plot of the Hall–Petch relationship for the friction stir welded Al bronze.

SZ in different areas is related to the smaller grain size. This is corroborated by the results of Afrin et al. (2008) which indicate the grain boundaries has become the main obstacle against slip of the dislocations so that the materials with a smaller grain size would show a greater hardness and strength as it would impose even more restriction to the dislocation movement. The linear Hall–Petch relationship (Park et al., 2003) could be written as $HV = 90.8 + 0.169d^{-1/2}$, where H and d are hardness (micro Vickers) and grain size (m) values, respectively. The result of hardness experiments was plotted as a function of grain size by the Hall–Petch relationship which is demonstrated in Fig. 9.

4. Conclusions

Microstructure evolution and mechanical properties of a friction stir welded casting of Cu–9Al–1Fe alloy were investigated. The main conclusions are listed below:

1. With a ω^2/v ratio going below 3×10^3 some weld defects were detected including cavity, lack of penetration and crack.
2. FSW refined the as-cast coarse microstructure in the base metal, and led to the formation of four distinct areas containing various coaxial grains within the SZ.
3. The α -phase grain size in FSW was dependent on the simultaneous effect of heat input and heat transfer rate during the welding process. Increasing the heat input and decreasing the heat transfer rate, could increase the grain size which was achieved by increasing the ω/v ratio.
4. Reduction of the ω/v ratio from 1500/50 to 1250/100, moved the areas of grain growth from the surface area (A) toward the sub-surface (B) and central (C) areas. Finer α -phase grain structures formed in the bottom areas (D), because of the low content of heat input in this area and the fact that the conditions of higher heat transfer rates were provided there.

5. The effect of grain size on microhardness in the stir zones was satisfied with Hall–Petch relationship.

References

- Afrin, N., Chen, D., Cao, X., Jahazi, M., 2008. Microstructure and tensile properties of friction stir welded AZ31B magnesium alloy. *Materials Science and Engineering: A* 472 (January (1–2)), 179–186.
- Arbegas, W.J., Hartley, P.J., 1998. Proceedings of the Fifth International Conference on Trends in Welding Research, Pine Mountain, GA, USA (June 1–5, 1998), [Properties_heavy_loaded_copper.701-4.pdf](#).
- Arbegas, W.J., 2008. A flow-partitioned deformation zone model for defect formation during friction stir welding. *Scripta Materialia* 58, 372–376.
- Callcut, V., 2002. Aluminum Bronzes. <http://www.copper.org/publications/newsletters/innovations/2002/08/aluminum2.html>
- Copper Development Association, 1988. *Welding Aluminium Bronze*. www.cda.org.uk.
- Fuller, M.D., Swaminathan, S., Zhilyaev, A.P., Mcnelley, T.R., 2007. Microstructural transformations and mechanical properties of cast NiAl bronze: effects of fusion welding and friction stir processing. *Materials Science and Engineering A* 463, 128–137, <http://dx.doi.org/10.1016/j.msea.2006.07.157>.
- Gadakh, V.S., Adepu, K., 2013. Heat generation model for taper cylindrical pin profile in FSW. *Journal of Materials Research and Technology* 2 (4), 370–375.
- Fuller, M.D., 2006. *Friction Stir Processing and Fusion Welding in Nickel Aluminum Propeller Bronze*. Distribution, Monterey, CA.
- Mishra, R.S., Mahoney, M.W., Bingel, W.H., Sharma, S.R., 2007. *Friction Stir Welding and Processing*.
- Ni, D.R., Xue, P., Wang, D., Xiao, B.L., Ma, Z.Y., 2009. Inhomogeneous microstructure and mechanical properties of friction stir processed NiAl bronze. *Materials Science and Engineering: A* 524, 119–128, <http://dx.doi.org/10.1016/j.msea.2009.06.013>.
- Ni, D.R., Xiao, B.L., Ma, Z.Y., Qiao, Y.X., Zheng, Y.G., 2010. Corrosion properties of friction–stir processed cast NiAl bronze. *Corrosion Science* 52 (5), 1610–1617, <http://dx.doi.org/10.1016/j.corsci.2010.02.026>.
- Oh-ishi, K., McNelley, T.R., 2004. Microstructural modification of as-cast NiAl bronze by friction stir processing. *Work* 35 (September), 2951–2961.
- Oh-ishi, K., McNelley, T.R., 2005. The influence of friction stir processing parameters on microstructure of as-cast NiAl bronze. *Work* 36 (June), 1575–1585.
- Park, S.H.C., Sato, Y.S., Kokawa, H., 2003. Microstructural evolution and its effect on hall–petch relationship. *Journal of Materials Science* 21, 4379–4383.